Confirmation of secondary cosmic ray flux enhancement during the total lunar eclipse of 10 December 2011

Anil Raghav,[1] Ankush Bhaskar,[2] Virendra Yadav,[2] Nitinkumar Bijewar,[1] Chintamani Pai,[1] Ashish Koli,[1] Nilam Navale,[1] Gurinderpal Singh,[1] Nitin Dubey,[1] Sushant Pawar,[1] Pradnya Parab,[1] Gandhali Narvankar,[1] Vaibhav Rawoot,[1] Vikas Rawat,[1] Satish Borse,[1] Nagnath Garad,[1] Carl Rozario,[1] Nitin Kaushal,[1] Shailendrakumar Tiwari,[1] and M. R. Press[1]

Received 16 May 2013; revised 29 August 2013; accepted 5 October 2013; published 24 October 2013.

[1] Temporal variation of secondary cosmic rays (SCR) flux was measured during the total lunar eclipse on 10 December 2011 and the subsequent full moon on 8 January 2012 from Mumbai (Geomagnetic latitude: 10.6°N), India. The measurements were done by using NaI (Tl) scintillation detector with energy threshold of 200 keV. The SCR flux shows approximately 8.1% enhancement during the lunar eclipse as compared to the average of pre- and post-eclipse periods. Weather parameters (temperature and relative humidity) were continuously monitored, and their correlations with temporal variation in SCR flux have been examined. The influences of geomagnetic field, interplanetary parameters, and tidal effect on SCR flux have been considered. Qualitative analysis of SCR flux variation indicates that local weather, interplanetary, and geomagnetic factors affecting SCR flux fail to explain the observed enhancement during the eclipse. Lunar tidal effect on magnetosphere and crust still remains a possible mechanism which needs to be investigated in detail. The enhancement during lunar eclipse and widely reported decrease during solar eclipses may unravel hitherto unnoticed factors modulating SCR flux.

Citation: Raghav, A., et al. (2013), Confirmation of secondary cosmic ray flux enhancement during the total lunar eclipse of 10 December 2011, *J. Geophys. Res. Space Physics*, *118*, 6426–6433, doi:10.1002/2013JA019007.

1. Introduction

[2] Our planet Earth is being constantly bombarded by high-energy particles from the Sun and galactic cosmic rays (GCR). Though the Earth's magnetic field provides a protective shield sustaining the life, high-energy GCR manage to reach the Earth and contribute to secondary cosmic rays (SCR) flux by interacting with the Earth's atmosphere and surface. SCR flux variations have been extensively studied for Solar Cycles, 27 days' cycle, diurnal variations, coronal mass ejections (CMEs) and solar eclipses [*Dorman*, 2009; *Cecchini et al.*, 2009]. SCR flux is known to vary with factors such as local weather parameters (temperature, pressure, and humidity), geomagnetic variations, interplanetary parameters, and tidal effects [*Dorman*, 2009]. Since 1995, SCR flux variation during solar eclipses has attracted attention and a typical decrease in SCR flux has been reported [*Bhattacharyya et al.*, 1997; *Kandemir et al.*, 2000; *Antonova et al.*, 2007; *Bhattacharya et al.*, 2010; *Nayak et al.*, 2010; *Bhaskar et al.*, 2011]. *Bhattacharyya et al.* [1997] have ascribed the decrease in SCR flux during solar eclipse to atmospheric cooling. *Chintalapudi et al.* [1997] have explained the decrease in γ ray and X ray flux as a result of blocking of the Sun by the Moon. *Bhaskar et al.* [2011] have ascribed observed decrease seen in scintillation detector measurements to the blocking of the Sun. Also, they have observed time delayed response in Geiger-Muller (GM) counter measurements, which they have attributed to the physical processes occurring in the atmosphere during the eclipse. In such solar eclipse studies, researchers have attempted to correlate weather parameters and geomagnetic variations with SCR flux to understand the underlying mechanism. Of these, the local weather parameters have been thought of as a major factor for the observed decrease as there is a rapid change in local weather parameters during a solar eclipse. Still the complete physical mechanism of the observed decrease remains unraveled. On the other hand, in 1967, Anand Rao had studied lunar and solar eclipses by monitoring variation in SCR flux using a Geiger-Muller (GM) counter. He had observed enhancements in SCR flux during the lunar eclipses [*Ananda Rao*, 1967]. Surprisingly, his work seems to have gone unnoticed as after him not much study of SCR flux variation was carried out during lunar eclipses. During a lunar eclipse, no variation in local weather parameters is expected. Hence, one does not expect any change in SCR flux during a lunar eclipse.

[1]Department of Physics, University of Mumbai, Bombay, India.
[2]Indian Institute of Geomagnetism, New Bombay, India.

Corresponding author: A. Raghav, Department of Physics, University of Mumbai, Vidyanagari, Santacruz (E), Mumbai-400098, India. (raghavanil1984@gmail.com)

2169-9380/13/10.1002/2013JA019007

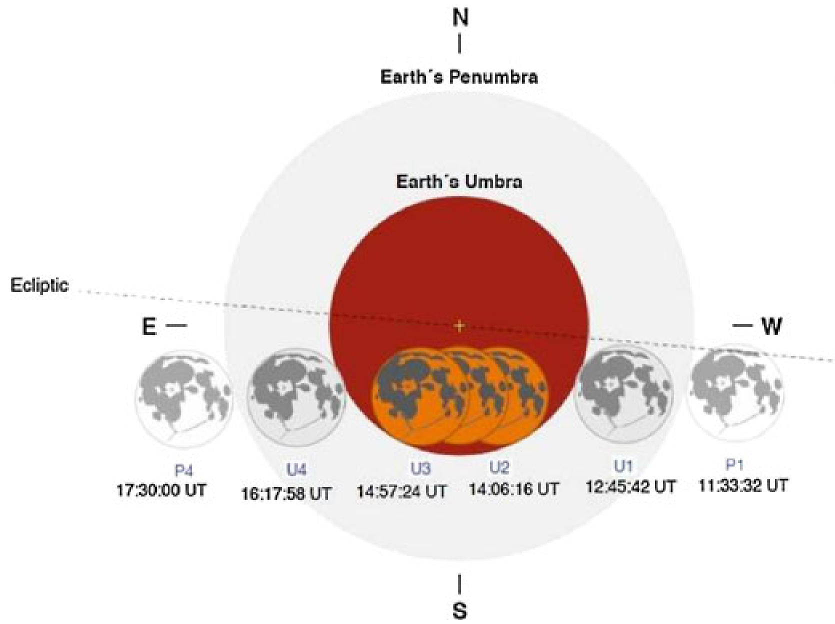

Figure 1. Geometrical and temporal parameters associated with the lunar eclipse of 10 December 2011, where P1, U1, U2, U3, U4, and P4 are the lunar contact timings with the Earth's Penumbra (P) and Umbra (U). (Eclipse map courtesy of Fred Espenak - NASA/Goddard Space Flight Center. See http://eclipse.gsfc.nasa.gov/eclipse.html for more information on solar and lunar eclipses).

Presumably, due to this reason, less attention has been given to SCR flux variation studies during lunar eclipses.

[3] Moreover, the unique geometrical alignment of the Sun, the Earth, and the Moon during an eclipse and effective tidal forces may be responsible for the observed phenomena during eclipses. The gravitational tidal forces due to the Moon can cause variations in atmosphere, ionospheric, and magnetospheric plasmas. Possible signatures of this in SCR flux have been reported in past studies. However, this is not yet well established. *Krymsky* [1994] has analyzed observations of the diurnal SCR variations in neutron and muon monitors. He has reported that the SCR variation with a period of half a lunar day could be explained by the lunar tidal effect in the atmosphere. *Dorman and Shatashvili* [1961] have noticed that during full moon, SCR flux is enhanced, whereas during new moon, a decrease is observed. They have explained this as a possible lunar tidal effect on the Earth's atmosphere and magnetosphere.

[4] *Volodichev et al.* [1991] have reported an intensity burst of thermal neutrons during the solar eclipse of 22 July 1990. Further, they have shown that thermal neutron enhancement occurs during new and full moon and the days close to them. They have ascribed the enhancement to the crossing of lunar tidal wave over their observation site which causes deformation of cracks in the Earth's crust. This releases trapped radioactive gases, mainly Radon, into the atmosphere. The alpha particles generated by Radon interact with the crust and the air, giving rise to the observed neutron splashes[*Volodichev et al.*, 1987, 1991, 1997; *Antonova et al.*, 2007].

[5] To confirm the enhancement of SCR during lunar eclipses and to investigate the underlying physical

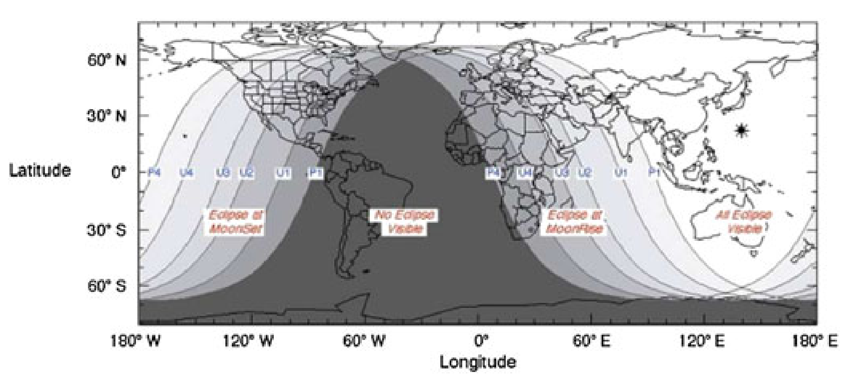

Figure 2. World map of the eclipse visibility: The dark area shows region having no eclipse visibility. (Eclipse map courtesy of Fred Espenak - NASA/Goddard Space Flight Center. For more information on solar and lunar eclipses, see http://eclipse.gsfc.nasa.gov/eclipse.html.).

Figure 3. Top view of NaI(Tl) scintillation detector used for the observations, which was kept inside lead shielding.

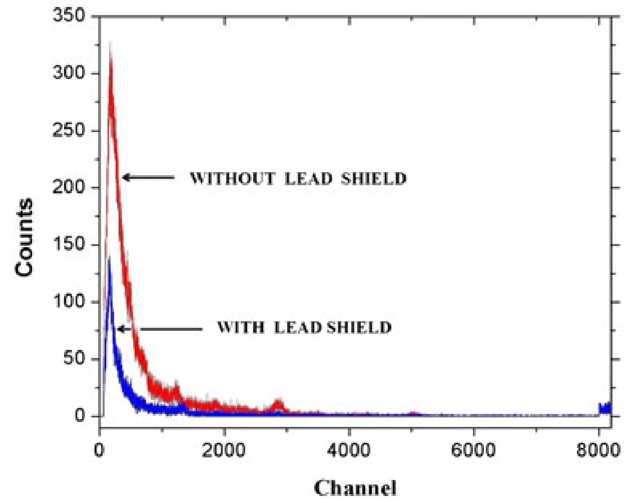

Figure 5. Background SCR spectrum with (blue) and without (red) lead shielding.

mechanisms, we have carried out SCR flux measurements during the total lunar eclipse on 10 December 2011 and the subsequent full moon (control day) on 8 January 2012 at the Department of Physics, University of Mumbai, Mumbai (Geomagnetic latitude: 10.6°N), India. Subsequent full moon day was purposely chosen as control day due to nearly similar positions of the Sun, the Moon, and the Earth as during a lunar eclipse. During this eclipse, the Moon's orbital trajectory took it through the southern half of the Earth's umbra. The total duration of the eclipse was about 5 h 56 min. Although the eclipse was not central, the total phase lasted for 51 min. The greatest eclipse occurred at 14:36 UT (http://eclipse.gsfc.nasa.gov/eclipse.html). The Moon's path through the Earth's shadows and a map illustrating worldwide visibility of the event is shown in Figures 1 and 2, respectively. Asia, Australia, and parts of Pacific had the best visibility. At the observing site, the Moon entered in penumbra before moonrise and exited before reaching its maximum altitude in the sky.

[6] This paper is arranged as follows: Section 1 includes motivation for the study and describes the eclipse parameters. The experimental setup is explained in section 2 of the paper. In section 3 we discuss our observations of temporal SCR flux variation during the total lunar eclipse and the subsequent control day. Section 4 presents weather conditions and their correlation with SCR flux variation on respective days. Geomagnetic and interplanetary conditions are discussed during both of the days in section 5. The tidal/gravitational effect is discussed in section 6. Section 7 concludes the paper with discussion and conclusions based on present investigation.

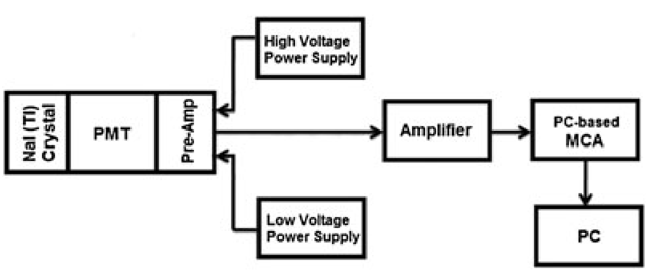

Figure 4. Schematic arrangement of the experimental setup used for the SCR flux measurement.

2. Experimental Setup

[7] A NaI (Tl) scintillation detector having dimensions of 7.62 cm × 7.62 cm was used to measure the variation of SCR flux during the eclipse. The detector was shielded by 5 cm thick lead bricks in a rectangular arrangement to minimize the background counts from the Earth and surroundings, allowing incoming SCR flux from top. The top view of the detector and lead shielding is shown in Figure 3. The detector signal generated by photo-multiplier tube (PMT) is processed through preamplifier (Pre-Amp), linear amplifier, multichannel analyzer (MCA) and then stored in a computer. A schematic arrangement of the setup is shown in Figure 4. The detector was calibrated at regular intervals during the observations using radioactive sources ^{137}Cs (0.662 MeV), and ^{60}Co (1.173 MeV, 1.332 MeV, and 2.505 MeV (sumpeak)).

[8] The SCR (secondary cosmic rays) flux was recorded with integration time of 10 min. To eliminate the possible low-energy noise from each spectrum, counts were summed up by keeping energy threshold of 200 keV. To quantify the effect of lead shielding, measurements of SCR flux were carried out when detector was shielded and unshielded well before the eclipse started [*Knoll*, 2000]. A significant reduction in the background counts was observed when the detector was shielded as shown in Figure 5. with unshielded detector, the data showed a background of approximately 87.0 counts per second, whereas with shielded detector, a background of approximately 19.8 counts per second was observed. During the eclipse, we observed maximum enhancement of 1.6 counts per second which suggests an increase of 8.1% over the average of pre- and post-eclipse data (see Figure 6a). In the absence of lead shielding, the enhancement would have been 1.8% (calculation considered the background count rate of 87 counts per second in case of no shielding) which is not significant. Hence, by arranging appropriate shielding, one can assure better

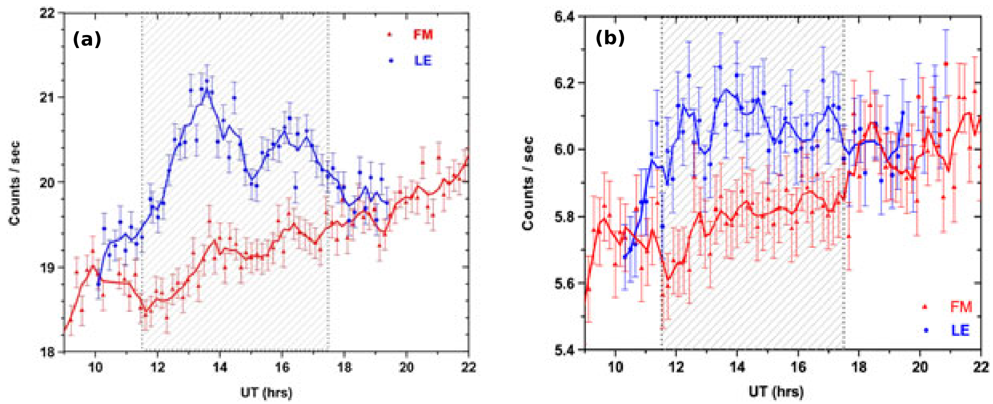

Figure 6. SCR flux variation with energy threshold of (a) 200 keV and (b) 800 keV during the lunar eclipse (LE) and control day (FM) as recorded by the scintillation detector. The trend line is two-point running average. The standard error is shown by vertical bars. Shaded region indicates eclipse duration and corresponding time interval on control day.

significance level of variation in SCR flux with respect to the average background [*Jackson and Welkar*, 2001].

3. Secondary Cosmic Ray Flux Variation

[9] Temporal variation of SCR flux during the lunar eclipse and the control day is shown in Figure 6. The variation in SCR flux on control day shows increasing trend. The observed enhancement in the SCR flux during the eclipse seems abnormal and unexpected as compared to the general trend of SCR flux on the control day. This enhancement coincides with the lunar entry and exit from the Earth's penumbra at P1 and P4, respectively, as shown in the shaded region. It shows approximately 8.1% enhancement in SCR flux during the lunar eclipse when compared to the average of pre- and post-eclipse counts. The maximum enhancement during the lunar eclipse is approximately 5σ, where σ is average standard error of control day counts corresponding to the eclipse duration. Thus, the observed enhancement is prominent. The statistical error bars are smaller as compared to the count rate which indicates that the observed enhancement is statistically significant. A double hump structure is clearly seen in SCR flux variation during the eclipse time interval, and amplitude of the first hump is higher as compared to the second. It is important to note that the SCR flux before the Moon's entry and exit from the Earth's penumbra converges to the control day SCR flux at corresponding times. As noted in section 1, Volodichev and group have observed enhancement in thermal neutron during full and new moon and the days close to them. They have ascribed it to the lunar tidal waves crossing over the observation site, which releases radioactive gases from the Earth's crust. These gases produce neutrons, which further decay into protons by emitting β particles. There is an upper limit to the energy of β particle emitted during neutron decay which is about 782 keV. To eliminate the possible contribution of the β particles produced by the proposed mechanism, the SCR flux was reestimated by keeping energy threshold of 800 keV. The reestimated flux variation is shown in Figure 6b. Due to the higher energy threshold, the counts are lower resulting in higher statistical uncertainty. After removing the possible contribution of the β particles, the enhancement is low, but still observable.

[10] To see the detector response and the stability of the detector, we ran the setup continuously from 13–17 November 2012 and again from 25 November 2012 to 6 December 2012. Calibration runs were performed at regular time intervals during the experiment. Data of each day were analyzed by keeping the fixed energy threshold (200 keV) during each day. To compare the day to day changes in baseline of SCR flux variation, the count rates were normalized with the average count rate between 23:00 and 24:00 (local time) of each day which is the least disturbed time of SCR diurnal variation. The average diurnal trend with standard deviation, obtained by using all 17 days' data counts at corresponding times, is shown in Figure 7. The shaded area in the figure corresponds to the eclipse duration which shows no large deviation.

4. Local Weather Parameters

[11] Ambient temperature and relative humidity were recorded at every 10 min during the eclipse and the control

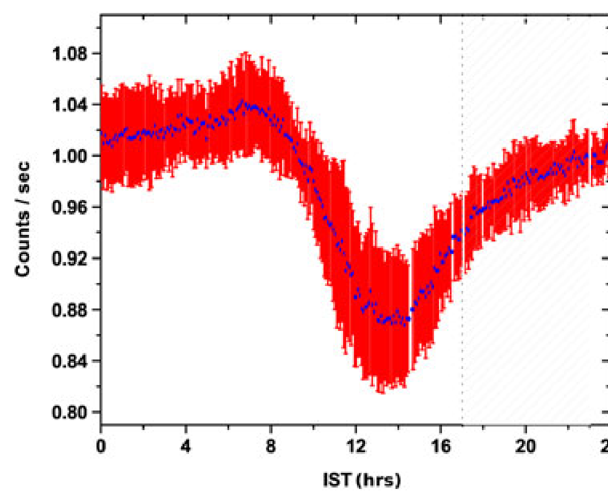

Figure 7. Average diurnal variation of SCR flux with standard deviation at the observation site. Abscissa is Indian Standard Time (IST). Shaded region indicates corresponding eclipse duration.

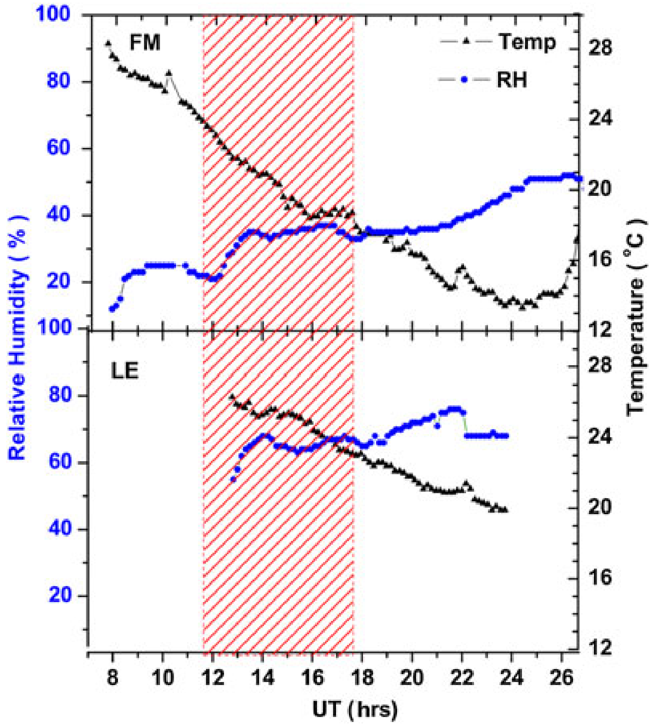

Figure 8. Temporal variation of weather parameters (temperature and relative humidity) during control day (FM) and eclipse day (LE). The temperature/relative humidity shows decreasing/increasing trend during eclipse period. This is due to day to night transition period at the observation site. Shaded region indicates eclipse duration and corresponding time interval on control day.

day using a digital temperature and humidity sensor. Figure 8 shows temporal variations of relative humidity and temperature during the control and the eclipse days. Shaded region indicates eclipse duration and corresponding time interval on control day. The diurnal patterns of temperature and relative humidity are clearly seen on both of the days. Though weather data is missing at the beginning of the eclipse, it is observed that during the eclipse, temperature steadily decreases from 26.4°C to 23.3°C and relative humidity increases from 55% to 67%. A similar trend is observed in both of the parameters on the control day during the same time interval. The average temperature/humidity is lower/higher on the control day as compared to the eclipse day. This is due to the control day being in January, which is generally cooler than December at the observing site. This assures no abnormal changes in the observed weather parameters during the eclipse.

[12] It is well known that SCR flux gets modulated by weather parameters in which temperature and humidity play an important role [*Lockwood and Yingst*, 1956]. In past studies, negative correlation between SCR flux and pressure was observed, whereas positive correlation between SCR flux and humidity was seen. The effect of temperature is not certain since the Earth's atmosphere is not isothermal, so it is difficult to quantify, but negative temperature effect on SCR flux is expected [*Olbert*, 1953; *Clay and Bruins*, 1939]. To investigate the effect of measured weather parameters, we have carried out correlation analysis between weather parameters and SCR flux for the eclipse and control days. The estimated Pearson and Spearman correlation coefficients are shown in Table 1 [*Spearman*, 1904; *Dorogovtsev et al.*, 2010; *Bhaskar et al.*, 2011].

[13] As expected, high negative correlation between temperature and relative humidity is observed on both of the days. On control day, the temporal variation in SCR flux is positively correlated with relative humidity and negatively correlated with temperature. Estimated correlation coefficients (greater than 90% confidence level) suggest, SCR flux negatively correlates with relative humidity and positively correlates with temperature during the eclipse. The observed correlations of SCR flux with weather parameters during the eclipse are opposite as compared to the control day which cannot be explained physically. It is important to note that though the two quantities show high positive correlation, there might not be a cause and effect relationship between them. Therefore, the observed enhancement in SCR flux during the lunar eclipse cannot be explained on the basis of variations in local weather parameters only.

5. Interplanetary and Geomagnetic Parameters

[14] The effects of interplanetary and geomagnetic parameters on SCR flux during the lunar eclipse and control days have been studied using interplanetary and geomagnetic indices data obtained from Coordinated Data Analysis Web (CDAWeb) database (http://cdaweb.gsfc.nasa.gov/). The neutron flux data is obtained from the Moscow Neutron Monitor station (http://helios.izmiran.rssi.ru/cosray/main.htm). Although this station did fall in the eclipse visibility region, SCR (neutron) flux shows no systematic variation during the eclipse. This can be correlated to SCR flux observed at the site during the eclipse and control days as seen in Figures 9b and 9b, respectively. The vertical component of interplanetary magnetic field (IMF B_z) fluctuates between southward and northward indicating small disturbance in interplanetary medium (see Figure 9a and 9a). The Symmetric-H (*SYM-H*) index is the strength of

Table 1. Correlation Coefficients of SCR Flux and Weather Parameters

Case	Correlation Between	Pearson Correlation Coefficient	Spearman Correlation Coefficient
Control day	Relative Humidity and SCR flux	0.92	0.90
	Temperature and SCR flux	–0.78	–0.78
	Relative Humidity and Temperature	–0.84	–0.87
Lunar Eclipse day	Relative Humidity and SCR flux	–0.52	–0.50
	Temperature and SCR flux	0.80	0.80
	Relative Humidity and Temperature	–0.73	–0.79

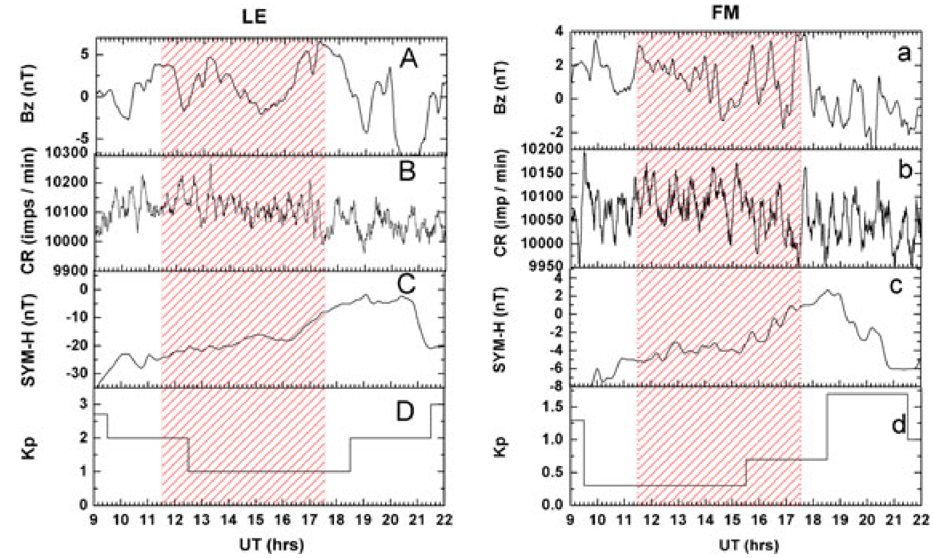

Figure 9. Interplanetary and geomagnetic parameters for (left column) eclipse day (LE) and (right column) control day (FM). (A, a) Vertical component of interplanetary magnetic field (IMF B_z). (B, b) Cosmic ray neutron flux (CR). (C, c) Symmetric component of the terrestrial ring current (*SYM-H*). (D, d]) Planetary 3 h range index (*Kp*). Shaded region indicates eclipse duration and corresponding time interval on control day.

symmetric ring current which encircles the Earth in the geomagnetic equatorial belt and generally gets intensified during prolonged southward B_z [*Wanliss and Showalter*, 2006, http://wdc.kugi.kyoto-u.ac.jp/aeasy/asy.pdf]. Figure 9c and 9c show temporal variation of the *SYM-H*. The *SYM-H* shows increasing trend during the eclipse indicating recovery phase of a weak geomagnetic storm. Though *SYM-H* was negative, it was less in amplitude ($\leq$ 30 nT) indicating minor geomagnetic disturbance [*Gonzalez et al.*, 1994]. Planetary *Kp* index remained low ($\leq$ 2) during the eclipse and during the control day assuring a geomagnetically quiet period [*Rajaram and Prisharoty*, 1998].

[15] The Moscow Neutron Monitor measures neutrons (produced by cosmic rays of 10–20 GeV) and the scintillation detector used in the present study measures SCR (0.2 MeV to ~4.5 MeV). The neutron monitor is located at high geomagnetic latitude, whereas the observations presented in this study were carried out at low geomagnetic latitude. Due to lower geomagnetic cutoff rigidity at high geomagnetic latitudes, one should expect much higher SCR flux over there as compared to low geomagnetic latitudes [*Thompson*, 1938]. In addition to all these, as explained earlier in section 2, lead shielding was used to minimize the surrounding background radiation. These differences result in the observed discrepancy between the observations from the two locations. Also, we do not see any correlated enhancement in muon monitors (e.g., Kuwait and Nagoya). Cosmic ray observatories generally measure cosmic ray flux (muons) in shower trigger mode to measure energy and direction of primary cosmic rays. The setup used in the present study measures overall secondary cosmic ray flux generated from primary cosmic rays of low to high energy range. Therefore, this setup allows us to detect variation of SCR flux irrespective of energy of primary cosmic rays. It is important to note that the physical phenomena reflected in low-energy primary cosmic rays will be missed out by high-energy cosmic ray observatories due to their trigger based high energy threshold. So one may not be able to observe similar enhancement in the cosmic rays observatories which are observing mainly high-energy primary cosmic rays. This might be a reason of absence of lunar eclipse signature in high-energy neutron or muon monitors. To investigate the relation between interplanetary and geomagnetic parameters with the observed SCR flux, correlation analysis has been performed. Results of the analysis are shown in Table 2. There is almost no correlation observed of SCR flux with B_z, *SYM-H* and neutron flux. On the control day, SCR flux shows weak negative correlation with B_z and Neutron flux whereas strong correlation with *SYM-H*. Thus, the absence of any systematic correlation of SCR flux with interplanetary

Table 2. Correlation Coefficients of SCR Flux With Interplanetary and Geomagnetic Parameters

Case	Correlation Between	Pearson Correlation Coefficient	Spearman Correlation Coefficient
	B_z and SCR flux	–0.22	–0.3
Control day	*SYM-H* and SCR flux	0.72	0.80
	Neutron flux and SCR flux	–0.13	–0.14
	B_z and SCR flux	0.02	–0.02
Lunar Eclipse day	*SYM-H* and SCR flux	0.04	0.18
	Neutron flux and SCR flux	0.11	0.14

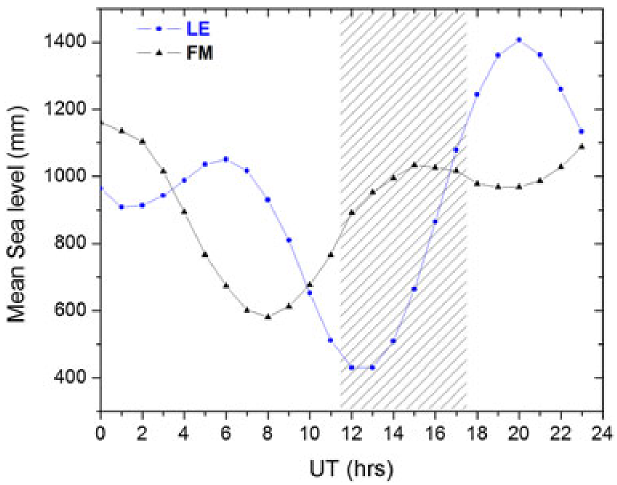

Figure 10. Temporal variation of mean sea level during the control day (FM) and the eclipse day (LE) at HANIMAAD station. Shaded region indicates eclipse duration and corresponding time interval on control day.

or geomagnetic parameters rules out the interplanetary or geomagnetic origin for the observed enhancement.

6. Tidal/Gravitational Effect

[16] The Moon and the Sun generate tidal waves in the Earth's magnetosphere, atmosphere, and oceans through gravitational interaction. Amplitude of the atmospheric tide increases with altitude so one can expect stronger tides in magnetospheric plasma which can modulate the SCR flux [*Mitra*, 1951; *Appleton and Weekes*, 1939]. At a distance r (expressed in terms of the Earth's radius) measured from the center of the Earth, the lunar tidal acceleration (a) will be

$$a = GM_{\mathrm{M}}/(R_{\mathrm{ME}} - r)^2 - GM_{\mathrm{M}}/(R_{\mathrm{ME}}^2) \approx 2rGM_{\mathrm{M}}/R_{\mathrm{ME}}^3 \qquad (1)$$

where, R_{ME} is the Moon-Earth distance and M_{M} is mass of the Moon [*Dorman*, 2009]. The tidal force is maximum when the Moon reaches the zenith/nadir of the observer, so high tide is generally observed when the Moon crosses the zenith/nadir. However, at the observing site, the Moon was closer to the horizon at the beginning of the eclipse, and the eclipse ended well before the Moon reached its maximum elevation in the sky. To demonstrate the lunar tidal variations on ground and compare them with the SCR flux observations, we have used mean sea level data as a proxy for tidal amplitude. Hourly mean sea level data is obtained from the University of Hawaii Sea Level Center (http://ilikai.soest.hawaii.edu/). We have used HANIMAAD station (Geog. Lat: 6°46′N, Geog. Long: 73°10′E) which is located close to Mumbai. Figure 10 shows the mean sea level variation on the eclipse and control days. In the beginning of the eclipse, mean sea level is low due to low tide and reaches the maximum approximately 1 h after the eclipse ends. It is important to note that the maximum enhancement seen in the SCR flux is not correlated with the mean sea level variation on any of the days.

[17] Also, the observed SCR flux enhancement during the lunar eclipse and decrease during solar eclipses discard the possibility of tidal effect by assuming the relative alignment of the Moon, the Earth, and the Sun. Therefore, the possibility of tidal effect to explain the decrement in SCR flux is ruled out.

7. Discussion and Conclusion

[18] As mentioned in section 1, there have been many observations of decrease in SCR flux during solar eclipses [*Bhattacharyya et al.*, 1997; *Chintalapudi et al.*, 1997; *Kandemir et al.*, 2000; *Bhattacharya et al.*, 2010; *Nayak et al.*, 2010; *Bhaskar et al.*, 2011]. During a solar eclipse, obscuration of the Sun by the Moon brings a rapid change in the intensity of solar radiation causing sudden changes in weather parameters which are generally believed to cause decrease in SCR flux. However, even the recent studies have failed to firmly establish the actual physical mechanism of the phenomenon [*Bhattacharya et al.*, 2010; *Nayak et al.*, 2010; *Bhaskar et al.*, 2011]. It is important to note that the reported observations of SCR flux during solar eclipses show positive correlation between the SCR flux variation and temperature, whereas the earlier studies on diurnal variation of SCR and meteorological effects on SCR show negative correlation with temperature [*Olbert*, 1953; *Lockwood and Yingst*, 1956]. As discussed in the previous section, even atmospheric lunar tidal effect does not seem to explain decrease in SCR during solar eclipses. Therefore, the decrease in SCR flux during a solar eclipse is still an unsolved mystery. Unlike solar eclipse induced modulation of SCR, lunar eclipse induced SCR modulation is unexpected due to the absence of any rapid change in weather parameters.

[19] The cosmic ray shadow effect of the Moon and the Sun (decrease in GCR flux due to the direct blocking of GCR by the Sun or the Moon) has been observed in GCR (in TeV energy regime) by using cosmic ray arrays [*Amenomori et al.*, 1993a, 1993b]. However, this decrease is always present irrespective of solar or lunar eclipse occurrence. This implies that shadow effect of the Moon seen in GCR cannot account for observed enhancement/reduction in the SCR flux during lunar/solar eclipses.

[20] *Dorman and Shatashvili* [1961] explained the decrease/increase of neutron flux during new moon/full moon as geomagnetic rigidity variation due to lunar tides in the magnetospheric plasma. This can be one of the possible mechanisms and needs to be explored in future studies.

[21] To investigate the proposed mechanism of neutron bursts observed during lunar eclipse and near full or new moon days, we have removed the β particle contribution from the SCR flux by keeping threshold of 800 keV. The β particles generated by neutron burst do not contribute in SCR flux of > 800 keV. Therefore, with this energy threshold, one should not expect any enhancement in SCR if the neutron burst mechanism is responsible for the observed enhancement. Even after removing β particle contribution, we do observe enhancement in SCR (see Figure 6b). This might indicate possibility of some other mechanism underlying the enhancement. However, one should not overlook that the observed enhancement (Figure 6b) is statistically less significant and less prominent as compared to the control day. So, the proposed mechanism of *Volodichev et al.* [1991] may be one of the possible mechanisms

underlying the observed enhancement of SCR flux during the eclipse [*Antonova et al.*, 2007; *Volodichev et al.*, 1991, 1987, 1997]. We recommend more detailed study to validate this observation.

[22] We have systematically ruled out the possibility of local weather, interplanetary, and geomagnetic parameters, which at first appeared to be the likely candidates causing the enhancement in SCR flux. This raises a possibility of tides in magnetospheric plasma, crustal deformation due to gravitational tides and some unknown parameter/parameters which is/are responsible for the observed enhancement.

[23] The upper atmospheric parameters are not available during this period, so one cannot neglect variations in upper atmosphere as another possible cause. It is also possible that the source causing SCR variation during eclipses lies even beyond the Earth's environment and may be associated with the Moon. For example, the crossing of the Moon through the Earth's magnetotail might be playing a role in modulating SCR flux.

[24] We believe that the present work reports the first observation of SCR flux variation during a lunar eclipse using a scintillation detector. Comparative study of the eclipse and control days indicates that the observed enhancement in SCR flux is unambiguous. However, at present, the underlying physical phenomenon is unknown and appears to have potential to initiate detailed work. We lay strong emphasis on more comprehensive studies during upcoming lunar eclipses to validate the present observations and investigate the underlying physical mechanism.

[25] **Acknowledgments.** We are thankful to WDC for Geomagnetism, Kyoto and CDAWeb for making interplanetary and geomagnetic data available. We are thankful to the Department of Physics, University of Mumbai, Mumbai for providing experimental resources and facilities. We extend our heartfelt thanks to S. M. Chitre, S. B. Patel, and S. K. Tandel of UM-DAE Center for Excellence in Basic Sciences, Mumbai for their constant encouragement and support. We would like to express our gratitude to A. A. Rangwala, D. C. Kothari, A. Misra, C. V. Gurada, and R. Srinivasan of the Department of Physics. We thank G. Rajaram, G. Vichare, D. Tiwari and B. Kakad of Indian Institute of Geomagnetism, Navi Mumbai. We are also thankful to all nonteaching staff of Department of Physics for their cooperation throughout the experiment. We are thankful to A. Patwardhan of St. Xavier's College, Mumbai. We thank Riddhi Kadrekar, Priya Pagare, Katharine Rowlins, Namrata Maladkar, Shraddha Chalke, Satish Vishwakarma, J. More, Bipin Sonawane, S. Kadam, and S. Sathian.

[26] Philippa Browning thanks Kazi Firoz and an anonymous reviewer for their assistance in evaluating this paper.

References

Amenomori, M., et al. (1993a), Direct evidence of the interplanetary magnetic field effect on the cosmic ray shadow by the Sun, *Astrophys. J.*, *415*, L147–L150.

Amenomori, M., et al. (1993b), Cosmic ray shadow by the moon observed with the Tibet air shower array, *23rd Int. Cosmic Ray Conf.*, *4*, 351–354.

Ananda Rao, J. N. (1967), Variation in the background counting rate at Tirupati during the periods of solar and lunar eclipses, *Phys. Lett. A*, *25*, 74–74.

Antonova, V. P., N. Volodichev, S. Kryukov, A. Chubenko, and A. Shchepetovet (2007), Effect of solar eclipse on neutron flux variations at the Earth's surface, *Bull. Russ. Acad. Sci. Phys.*, *71*, 1054–1057.

Appleton, E. V., and K. Weekes (1939), On lunar tides in the upper atmosphere, *Proceedings of the Royal Society of London. Series A, Mathematical and Physical Sciences*, *171*, 171–187.

Bhaskar, A., et al. (2011), A study of secondary cosmic ray flux during the annular eclipse of 15 January 2010 at Rameswaram, India, *Astropart. Phys.*, *35*, 223–229.

Bhattacharyya, A., et al. (1997), Variation of gamma ray and particle fluxes at the sea level during the total solar eclipse of 24 October, 1995, *Astro. Space Sci.*, *250*, 313–326.

Bhattacharya, R., M. Roy, M. Biswas, R. Guha, and A. Bhoumick (2010), Cosmic ray intensity and surface parameters during solar eclipse on 22 July 2009 at Kalyani in West Bengal, *Curr. Sci.*, *98*, 1609–1614.

Cecchini, S., et al. (2009), Time variations in the deep underground muon flux, *Europhys. Lett.*, *87*, 39001.

Chintalapudi, S. N., V. Ghosh, J. B. M Krishna, J. R. Verman, H. Prakash, G. Pal, N. R. Mishra, M. Bera, V. R. Reddy, and M. R. Ranganath (1997), γ and X ray measurements during total solar eclipse on October 24, 1995 at Diamond Harbour, *Kodaikanal Obs. Bull.*, *13*, 225–234.

Clay, J., and E. M. Bruins (1939), Variations of cosmic ray intensity with variation of barometric pressure and temperature at sea level, *Rev. Mod. Phys.*, *11*, 158–159.

Dorman, L. I., and L. Kh. Shatashvili (1961), Lunar-daily variation of cosmic ray neutron component and the prolem on its origin, *Geomagn. Aeron.*, *1*, 663–670.

Dorman, L. I. (2009), *Cosmic Rays in the Magnetosphere of the Earth and Other Planets*, Astrophysics and Space Science Library, Springer.

Dorogovtsev, S. N., A. L. Ferreira, A. V. Goltsev, and J. F. F. Mendes (2010), Zero Pearson coefficient for strongly correlated growing trees, *Phys. Rev. E.*, *81*, 031135.

Gonzalez, W. D., J. A. Joselyn, Y. Kamide, H. W. Kroehl, G. Rostoker, B. T. Tsurutani, and V. M. Vasyliunas (1994), What is geomagnetic storm?, *J. Geophys. Res.*, *99*, 5771–5792.

Jackson, D. P., and M. T. Welkar (2001), Measuring and modeling cosmic ray showers with an MBL system: An underground project, *Am. J. Phys.*, *69*, 896–900.

Kandemir, G., M. C. Guclu, M. Geckinli, C. Firat, S. Boydag, and A. Ozguc (2000), Variation of cosmic ray intensity during the solar eclipse August 11, 1999, *ASP Conf. Series*, *205*, 202–207.

Knoll, G. F. (2000), *Radiation Detection and Measurement,* 3rd ed., pp. 757–775, John Wiley, Chichester, UK.

Krymsky, G. F. (1994), On the lunar-daily cosmic ray variation, *Trudy YaFAN*, *4*, 108–110.

Lockwood, J. A., and H. E. Yingst (1956), Correlation of meteorological parameters with cosmic-ray neutron intensities, *Phys. Rev.*, *104*, 1718–1722.

Mitra, A. P. (1951), Solar tides in the ionosphere over Calcutta, *J. Atmos. Solar-Terr. Phys.*, *1*, 286–295.

Nayak, P. K., S. K. Gupta, A. Jain, I. Mazumdar, S. Raha, S. K. Saha, A. V. Bobrov, A. Osipov, and B. Shwartzet (2010), A study of gamma ray flux during the total solar eclipse of 1 August 2008 at Novosibirsk, Russia, *Astropart. Phys.*, *32*, 286–293.

Olbert, S. (1953), Atmospheric effects on cosmic-ray intensity near sea level, *Phys. Rev.*, *92*, 454–461.

Rajaram, G., and P. R. Prisharoty (1998), *The Earth's Magnetic Field*, pp. 146–147, Oxford and IBH Publishing Co. Pvt. Ltd., New Delhi.

Spearman, C. (1904), The proof and measurement of association between two things, *Am. J. Psychol.*, *15*(1), 72–101.

Thompson, J. (1938), Solar diurnal variation of cosmic-ray intensity as a function of latitude, *Phys. Rev.*, *54*, 93–96.

Volodichev, N. N., O. Yu. Nechaev, M. I. Panasyuk, and P. I. Shavrin (1987), Neutron beta-decay contribution to soft-electron intensity in the atmosphere, *20th Intern. Cosmic Ray Conf. Moscow. Nauka*, *4*, 266–268.

Volodichev, N. N., B. M. Kuzhevskij, O. Yu. Nechaev, M. I. Panasyuk, and P. I. Shavrin (1991), Strong increase of neutron flux during 22 July, 1990 Eclipse, *Proc 22nd ICRC (Dublin, Irelland, 11–23 August, 1991)*, *3*, 689–692.

Volodichev, N. N., B. M. Kuzhevskij, O. Yu. Nechaev, M. I. Panasyuk, and P. I. Shavrin (1997), Phenomenon of neutron intensity burst during new and full moons, *Cosmic Res.*, *35*, 135–143.

Wanliss, J. A., and K. M. Showalter (2006), High-resolution global storm index: *Dst* versus *SYM-H*, *J. Geophys. Res.*, *111*, A02202, doi:10.1029/2005JA011034.